Time response of the water table and saltwater transition zone to a base level drop

Y. Kiro,[1,2] Y. Yechieli,[1] V. Lyakhovsky,[1] E. Shalev,[1] and A. Starinsky[2]

Received 10 December 2007; revised 11 July 2008; accepted 26 September 2008; published 30 December 2008.

[1] This paper investigates the effect of a drainage base level drop on the groundwater system in its vicinity, using theoretical analysis, simulations, and field data. We present a simple and novel method for analyzing the effect of a base level drop by defining two characteristic times that describe the response of the water table and the transition zone between the fresh and saline water. The Dead Sea was chosen as a case study for this process because of the lake's rapid level drop rate. During a continuous lake level drop, the discharge attains a constant value and the hydraulic gradient remains constant. We describe this new dynamic equilibrium and support it by theoretical analysis, simulation, and field data. Using theoretical analysis and sensitivity tests, we demonstrate how different hydrological parameters control the response rate of the transition zone to the base level drop. In some cases, the response of the transition zone may be very rapid and in equilibrium with the water table or, alternatively, it can be much slower than the water table response, as is the case in the study area.

Citation: Kiro, Y., Y. Yechieli, V. Lyakhovsky, E. Shalev, and A. Starinsky (2008), Time response of the water table and saltwater transition zone to a base level drop, *Water Resour. Res.*, *44*, W12442, doi:10.1029/2007WR006752.

1. Introduction

[2] Understanding the effect of sea or lake level changes on groundwater is very relevant to the expected global sea level changes in the future and their consequences with regard to water management. The relation between lakes and groundwater has been studied widely [e.g., *Sacks et al.*, 1992; *Winter*, 1978], and the effect of lake level changes on the groundwater levels [*Anderson and Cheng*, 1993; *Cherkauer and Zager*, 1989] and on the fresh-saline interface have been observed in the field [*Yechieli*, 1993]. The effect of sea level changes on the groundwater levels and on the fresh-saline interface in a confined aquifer has also been tested in simulations using sharp interface models [e.g., *Essaid*, 1990; *Harrar et al.*, 2001; *Meisler et al.*, 1985] and density-dependent flow models [*Ataie-Ashtiani et al.*, 1999; *Chen and Hsu*, 2004]. However, the transition zone between the fresh and saline water has not been monitored over a period of time during a lake level drop. Furthermore, the various effects of a base level drop on fresh and saline water and the numerous parameters involved have not been studied in a rigorous manner.

[3] Studies on confined aquifers show that the transition zone is not always in equilibrium with the contemporary sea or lake level and there is a time lag between the groundwater level response and the transition zone response [*Essaid*, 1990; *Harrar et al.*, 2001; *Meisler et al.*, 1985; *Rogers and Dreiss*, 1995; *Yechieli*, 1993]. Analytical and numerical models [*Harrar et al.*, 2001] show that the groundwater level response depends on the hydraulic diffusivity ($D = T/S$ where T is transmissivity [$m^2\ s^{-1}$] and S is storativity). *Bush* [1988] has shown that lateral permeability, transverse dispersivity, and boundary lateral inflow have the largest influence on saline water movement. Furthermore, during a density-dependent flow, the density gradient has a major effect on the transition zone movement. Therefore wide transition zones, caused by large dispersivities, move relatively slowly [*Voss*, 1999].

[4] A drainage base level drop is likely to widen the transition zone because of the effect of the longitudinal dispersivity during vertical movement of the transition zone [*Meisler et al.*, 1985; *Underwood et al.*, 1992]. Ocean level changes that cause vertical movement of the transition zone may induce a wide transition zone. The widening of the transition zone due to vertical movement can occur over large timescales, as in global sea level changes [*Meisler et al.*, 1985], or small timescales, as in tides [*Ataie-Ashtiani et al.*, 1999; *Chen and Hsu*, 2004; *Underwood et al.*, 1992].

[5] The occurrence of a fresh-saline water interface is due to density differences between the fresh and saline water bodies. The location of the interface can be estimated by the Ghyben-Herzberg approximation, assuming that both the saline and fresh waters are stagnant. The sharp-interface approach is a good approximation when dealing with large spatial scales and when investigating general interface movement. *Cooper* [1959] has found from field data that the interface is not sharp, but is rather a transition zone between the fresh and saline water, known as the zone of dispersion. Because of the hydrodynamic dispersion, some of the saline water mixes with the fresh water, causing continuous seaward outflow of saline water, which drives saline water circulation beneath the transition zone [*Kohout*, 1960].

[6] Under transient conditions, the saline water circulation is more complicated. *Michael et al.* [2005] have shown

[1]Geological Survey of Israel, Jerusalem, Israel.
[2]Institute of Earth Sciences, Hebrew University of Jerusalem, Jerusalem, Israel.

0043-1397/08/2007WR006752$09.00

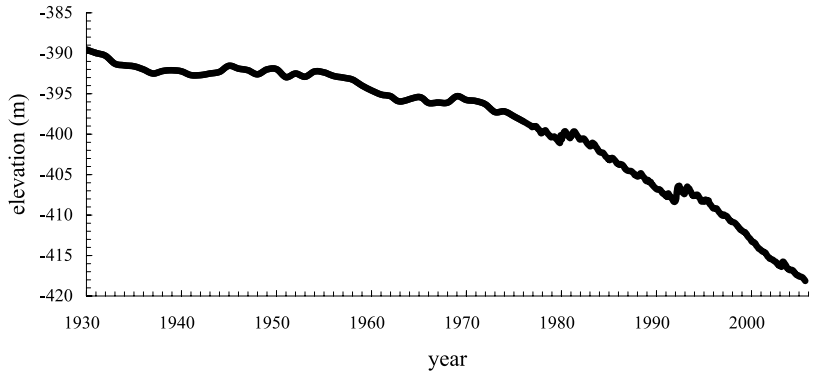

Figure 1. The Dead Sea levels since 1930 (modified after *Klein and Flohn* [1987]). Data from the Hydrological Service of Israel.

that changes in the hydraulic gradient that are caused by seasonal changes can affect the saline water flow beneath the transition zone. They showed that there is seaward outflow of saline water that is not compensated by inflow of saline water. They further showed that it could be caused by transition zone movement toward the sea that is due to an increase in the hydraulic gradient.

[7] The Dead Sea was chosen as a case study for investigating the response of the fresh and saline groundwater due to its fast rate of continuous base level drop. The Dead Sea level has been dropping during the past 50 years due to human influences [*Anati and Shasha*, 1989; *Klein and Flohn*, 1987], reaching a rate of 1 m a^{-1} in the last few years (Figure 1). This rapid drop in the Dead Sea level has a major effect on the groundwater system, providing a unique opportunity to study these processes. The characteristics of the Dead Sea region (Figure 2), its accessibility, and the fast drop of the lake level enable efficient monitoring of the groundwater system related to the effect of a lake level drop. The fact that the Dead Sea is a terminal lake whose level is almost unaffected by tides, waves, or global sea level changes isolates the effect of the lake level drop on the groundwater.

[8] The present study identifies processes that occur in time and space during a lake level drop and quantifies the response of the groundwater system. This study examines a phreatic aquifer close to the shore during a continuous base level drop. We develop a simple method for quantifying the fresh and saline groundwater responses that could be applied to any region given a set of parameters. We present a thorough study and quantification of the effect of a large set of aquifer parameters and boundary conditions. Unlike previous studies [*Essaid*, 1990; *Harrar et al.*, 2001; *Meisler et al.*, 1985], which used a sharp interface model, the small scale of the Dead Sea domain and its salinity distribution [*Kiro*, 2006] require a density-dependent model.

[9] The drop of the Dead Sea lake level provides a unique opportunity to study the effect of a base level drop in the field, in conjunction with theoretical analysis and hydrological numerical simulations. The combination of all three viewpoints provides a substantiated understanding of this process.

[10] In section 3 of this paper we analyze the case of an instantaneous base level drop and its effect on the water table and on the transition zone. For each property a theoretical analysis is presented, defining a characteristic time, followed by validation using the U.S. Geological Survey (USGS) SUTRA simulation code [*Voss*, 1984]. In section 4 we extend our analysis to the case of a continuous base level drop. In section 5 the theoretical study is applied to the Dead Sea region and compared with field data.

2. Hydrogeology

[11] The Dead Sea is a terminal lake (Figure 2) situated in the deepest part of the Dead Sea Transform. The Dead Sea region consists of two main aquifers: the Upper Cretaceous Judea Group aquifer and the Quaternary alluvial aquifer [*Arad and Michaeli*, 1967; *Yechieli et al.*, 1995]. The present study was carried out in the alluvial aquifer, which consists mainly of clastic sediments deposited in fan deltas (gravel, sand, and clay) and lacustrine sediments (clay, aragonite, gypsum, and salt). Alternations between gravel and clay create several subaquifers that differ in their groundwater level and chemical composition. This aquifer is bounded by normal faults, which set Cretaceous carbonate rocks of the Judea Group against Quaternary alluvial and lacustrine sediments. The recharge of the aquifer is through lateral flow from the Judea Group aquifer, which is replenished in the highlands 10–30 km to the west and by flash floods. Direct rain is negligible because of the arid climate and high evaporation in the Dead Sea region. The annual water volume that enters the Dead Sea today is $265-335 \times 10^6$ m^3, about half of which is from groundwater [*Lensky et al.*, 2005]. There is a hydraulic relationship between the Dead Sea and the adjacent groundwater system, expressed in a relatively rapid (a few days) water level response to level changes in the Dead Sea [*Yechieli et al.*, 1995].

[12] The Dead Sea salinity and density are 340 g L^{-1} and 1.24 kg L^{-1}, respectively. The extremely high density of the Dead Sea induces a very shallow transition zone between the fresh and saline water. According to the Ghyben-Herzberg approximation, the depth of the transition zone is 4.35 times the groundwater elevation compared with 40 times in the ocean [*Yechieli*, 2000].

3. Groundwater Response to an Instantaneous Base Level Drop

[13] In order to quantify the response of the groundwater system to a lake level drop, we first examined the response to an instantaneous drop by means of theoretical analysis,

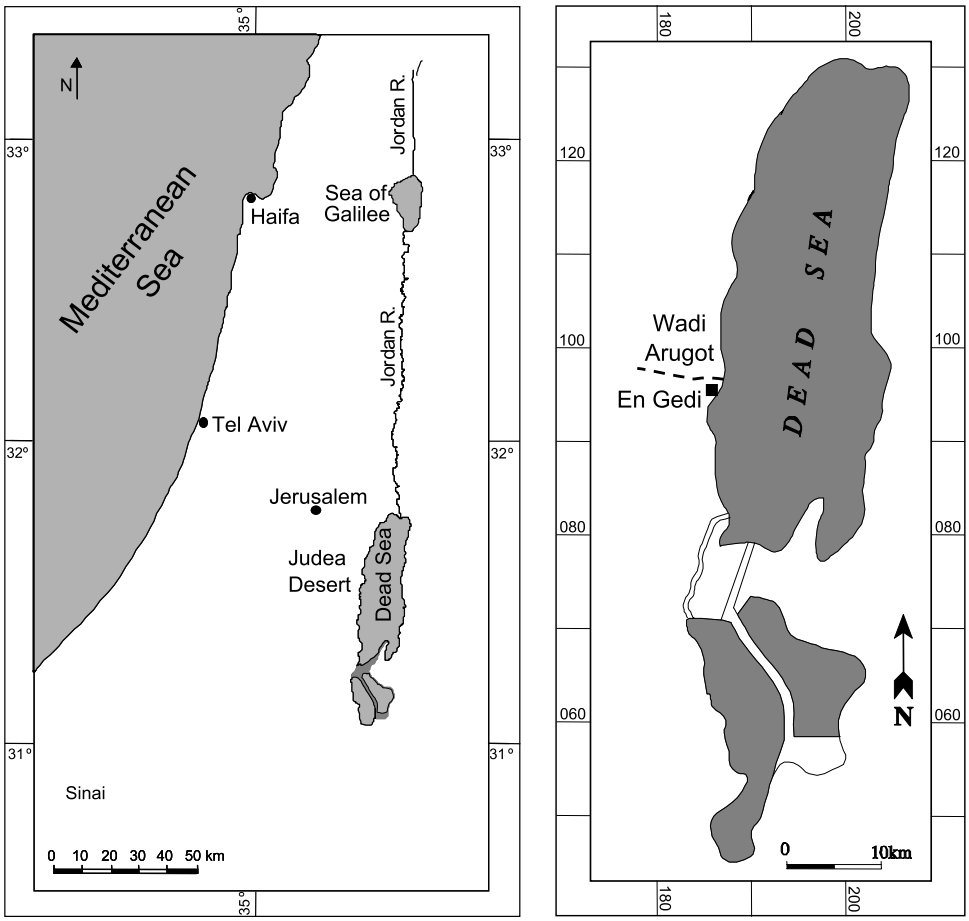

Figure 2. Location map of the Dead Sea and Wadi Arugot.

followed by validation using simulations with the SUTRA model. The response of the groundwater system involves two aspects, namely, the water table response and the transition zone response. It has been stated in previous studies, based on simulation and field data, that the transition zone responds much more slowly than the groundwater level [*Essaid*, 1990; *Harrar et al.*, 2001]. However, the results presented below show that in some cases the transition zone responds relatively rapidly and is almost in equilibrium with the moving water table.

3.1. Water Table Response

3.1.1. Theoretical Analysis

[14] The mass conservation equation in a phreatic aquifer consisting of only fresh water can be simplified by linearization, yielding a one-dimensional diffusion equation [*Bear*, 1979]:

$$\frac{\partial h}{\partial t} = \frac{T}{n}\frac{\partial^2 h}{\partial x^2}, \tag{1}$$

where h [m] is the deviation of the thickness of the flow section from the constant value, $h_0 \gg h$. The h is a function of the distance from the shore x [m] and time t [s], T [m^2 s^{-1}] is the transmisivity, and n is the porosity. Since the alluvial aquifer in the Dead Sea region is bounded by a normal fault, we assume a finite aquifer length L [m]. Thus the boundary and initial conditions are

$$h(0,t) = \Delta h; \quad \frac{\partial h}{\partial x}(L,t) = \frac{Q_0}{T}; \quad h(x,0) = \frac{Q_0}{T}x,$$

where Δh [m] is the magnitude of the instantaneous base level drop and Q_0 [m^2 s^{-1}] is the inflow.

[15] The solution of (1) with these boundary and initial conditions can be obtained by separation of variables in the form of a Fourier series [*Crank*, 1975]:

$$h(x,t) = \frac{Q_0}{T}x + \Delta h - 2\Delta h \sum_{k=0}^{\infty} \frac{1}{\pi/2 + \pi k} \sin\left(\frac{\pi/2 + \pi k}{L}x\right) \cdot \exp\left(-\frac{T}{nL^2}(\pi/2 + \pi k)^2 t\right), \tag{2}$$

The outflow rate at $x = 0$ according to Darcy's law is

$$Q(0,t) = Q_0 + \frac{2Kh_0\Delta h}{L} \sum_{k=0}^{\infty} \exp\left(-\frac{T}{nL^2}(\pi/2 + \pi k)^2 t\right), \tag{3}$$

where Q [m^2 s^{-1}] is the discharge, K [m s^{-1}] is the hydraulic conductivity, and h_0 [m] is the flow section thickness. The outflow at $x = 0$ as a function of time

Table 1. Simulation Boundary and Initial Conditions

Boundary	Condition
Eastern boundary	constant pressure; density and salinity of the Dead Sea
Western boundary	constant freshwater inflow
Upper boundary	no flow
Lower boundary	no flow
Initial conditions	level drop at the eastern boundary; water table and transition zone in steady state

indicates the rate of the fresh water body response, since the length of the aquifer (L) and the volume of discharged water are finite.

[16] On the basis of scaling analysis of equation (1), a characteristic time for the water table response (τ_{gw}) can be defined. After each perturbation the aquifer, with length L, is expected to return to the steady state flow pattern with a characteristic time scale of $\tau_{gw} = nL^2/T$. Equation (3) provides a mathematical expression for this process. Each term of the Fourier series (3) exponentially decays with time. For time $t = \tau_{gw}$, the decay of the discharge of the kth term is equal to $\exp(-(\pi/2 + \pi k)^2)$.

[17] The length of the aquifer was taken as the characteristic length (L) since the recharge is from the western boundary. Other settings may have other characteristic lengths, such as the distance to the hydraulic watershed or the distance to a natural boundary. In contrast to problems with an infinite aquifer length, in which the characteristic length is typically chosen as the length up to negligible groundwater level changes, the aquifer length in this case is finite, and hence every point within the aquifer will eventually be affected.

[18] In order to evaluate the significance of the linearization, a SUTRA simulation consisting of only fresh water was performed. The boundary conditions are given in Table 1. Neglecting the rainfall recharge for the Dead Sea area, the upper boundary of the simulated area is defined as no-flow. Note that SUTRA solves the problem in both saturated and unsaturated zones. The moving water table is an internal boundary between saturated and unsaturated zones where the hydraulic pressure is equal to zero. The simulated discharge is presented in Figure 3. The difference between the solutions stems from the linearization in (1) [*Bear*, 1972]. The neglected term $(\partial h/\partial x)^2$ leads to some deviation between the numerical and analytical solutions, while the shape of the discharge decrease is very similar. Therefore, in the next section we will use the functional form (3) in search for the correct timescale.

3.1.2. Simulations

[19] In order to reinforce the theoretical analysis and examine whether the transition zone affects the fresh water response, sensitivity tests were conducted with SUTRA examining τ_{gw} as a function of the boundary conditions and the aquifer parameters. The parameters that were tested are given in Tables 2 and 3. In addition to the parameters in (1), the governing equations of SUTRA require other parameters. These include the fluid and the porous matrix compressibilities, used for calculating the specific storativity, and the permeability, used instead of the hydraulic conductivity. The parameter values used are typical to phreatic aquifers. The aquifer dimensions were taken as the Dead Sea region dimensions, while the lengths were expanded by up to an order of magnitude. The inflow values were varied to produce different hydraulic gradients, while maintaining a phreatic aquifer for a given hydraulic conductivity.

[20] The fresh water discharge and the hydraulic gradient increase instantaneously as the lake level drops (Figures 3, 4a, and 4b). Following this initial increase, the hydraulic gradient decreases to its initial value and the discharge decreases to the inflow value, until a new equilibrium is attained (Figure 4c, Figure 3). The saline water circulates beneath the transition zone in steady state but as the base level drops it flows toward the lake (Figure 4b). When the transition zone is close to equilibrium, the saline water circulation appears again as it occurs in steady state (Figure 4c). The sudden drop can cause a temporary seepage face during the first month, which is accounted for in the total discharge.

[21] The main volume of the water discharge consists of fresh water. Therefore we assume that the discharge may be approximated using the functional form (3) with corrected values for A [$m^2\ s^{-1}$] and τ_{gw} [s]:

$$Q(0,t) = Q_0 + A\sum_{k=0}^{\infty} e^{-(\pi/2+\pi k)^2 \frac{t}{\tau_{gw}}}. \quad (4)$$

According to (3), τ_{gw} should be proportional to $nL^2/K_{\max}h_0$ where the transmisivity is $T = K_{\max}h_0$, the parameter $K_{\max}$[m s^{-1}] is the maximal hydraulic conductivity, and h_0[m] is the thickness of the flow section. A should be

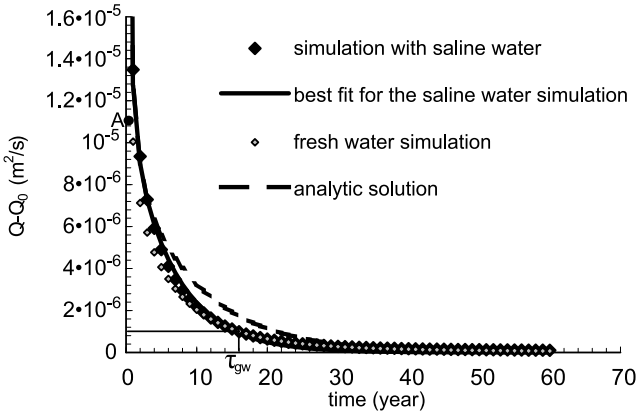

Figure 3. Change in the discharge to the Dead Sea ($Q - Q_0$) after an instantaneous level drop: analytic solution (first 1000 terms); fresh water simulation with parameters of the base simulation (Table 2); simulation including a transition zone (Table 2) and its best fit for the parameters A and τ_{gw}. The characteristic time is approximately the time in which the discharge decayed to $1/\exp(\pi^2/4)$ of its initial value (A).

Table 2. Hydrological Parameters of Simulations and Corresponding Predicted Values for Characteristic Times[a]

	Parameter	Unit	Value
α	aquifer compressibility	$[kg/(m\ s^2)]^{-1}$	10^{-7}–10^{-10} (10^{-10})
β	fluid compressibility	$[kg/(m\ s^2)]^{-1}$	4.47×10^{-10}
S	storativity		1.05×10^{-3} to 9.52×10^{-3} (1.99×10^{-4})
μ	fluid viscosity	$kg\ (m\ s)^{-1}$	0.001
ρ_0	freshwater density	$kg\ m^{-3}$	1000
C_0	freshwater concentration		0
ρ	groundwater density	$kg\ m^{-3}$	$\rho = \rho_0 + \partial\rho/\partial C(C - C_0)$
$\partial\rho/\partial C$	density change with concentration		836
	saline water concentration		0–0.275 (0.275)
ρ_s	saline water density		1000–1230 (1230)
n	porosity		0.1–0.3 (0.2)
L	aquifer length	m	2000–5000 (2000)
h_0	flow section thickness	m	40–120 (90)
Δh	lake level drop	m	1–20 (10)
Q_0	inflow	$m^2\ s^{-1}$	8.2×10^{-7} to 2.5×10^{-5} (8.2×10^{-6})
k_{max}	maximal permeability	m^2	10^{-13} to 7×10^{-12} (10^{-12})
k_{min}	minimal permeability	m^2	5×10^{-15} to 3.5×10^{-13}
K_{max}	maximal hydraulic conductivity	$m\ s^{-1}$	9.8×10^{-7} to 7×10^{-5} (9.91×10^{-6})
K_{min}	minimal hydraulic conductivity	$m\ s^{-1}$	4.9×10^{-8}–3.5×10^{-6} (4.955×10^{-7})
K_{max}/K_{min}	anisotropy		10–200 (20)
α_L	longitudinal dispersivity	m	5–100 (10)
α_T	transverse dispersivity	m	0.008–1 (0.01)
τ_{gw}	water table characteristic time	year	2–706 (15.75)
τ_{TZ}	transition zone characteristic time	year	4–53 (10)

[a]Sensitivity test base simulation values are given in parentheses. The values were taken from the references given in Table 4 as well as from field data and previous studies on the Dead Sea.

proportional to $2K_{max}h_0\Delta h/L$. The best fit between the simulation results and (4) yields the following relations:

$$\tau_{gw} = \frac{nL^2}{K_{max}h_0} \cdot F$$
$$A = \frac{2K_{max}h_0\Delta h}{L} \cdot M, \quad (5)$$

where F and M are dimensionless factors. Factor F had an approximately constant value of 0.55 in the different simulations mostly because of the linearization. Factor $M \approx \rho_s/\rho_0$, where ρ_s [kg m^{-3}] and ρ_0 [kg m^{-3}] are the saline and fresh water densities, respectively. This factor is due to the larger hydraulic gradient when taking into account the saline water body. Figure 5 shows the correspondence between parameters A and τ_{gw} as calculated by (5) and those obtained from the simulations. Equation (5) enables calculating the characteristic time of a system for any given set of parameters. Owing to the equation's theoretical basis, they are transferable to other regions, applying only minor assumptions.

[22] The factors F and M are calculated for the case of a phreatic aquifer where the recharge is from the western boundary. In most simulations we used an aquifer length (L) that is typical of the Dead Sea alluvial aquifer and the density of the lake (ρ_s) was set to the Dead Sea density. A few simulations were done with varying lake density values, ranging from freshwater to Dead Sea water. These simulations indicate that F is invariant to lake density and M is equal to the density ratio (ρ_s/ρ_0), as described above.

3.2. Transition Zone Response

[23] The transition zone response was analyzed by the same sensitivity tests (Tables 2 and 3) using the SUTRA model that was used in the fresh water response analyses. Because the transition zone response is a more complex problem (two-dimensional and affected by many parameters), the analysis was done using only the simulations. The results of the sensitivity tests show that the transition zone response differs from that of the water table and depends on τ_{gw}, the hydraulic gradient, which is given by the hydraulic conductivity and the inflow, and on the dispersivity.

[24] The response of the transition zone depends on τ_{gw}, but as the flow is density-dependent, it also depends on the density gradient [*Voss*, 1999]. Since the flow is approximately horizontal, the main effect is due to the horizontal component of the density gradient. Thus the slope of the transition zone affects its response rate since a small transition zone slope causes a small horizontal density gradient. Hence the hydraulic gradient that affects the transition zone slope according to Ghyben-Herzberg has a significant effect on the response rate of the transition zone.

[25] In order to quantify the response of the transition zone we examined the circulation of the saline water. According to the dispersive transition zone model [*Cooper*, 1959], the saline water circulates beneath the transition zone in steady state. The simulations of the present study show that saline water velocities are dominated by the dispersivities, anisotropy, and hydraulic conductivity, whereby high dispersivity, low anisotropy, and high hydraulic conductivity cause faster circulation.

[26] During a lake level drop, the saline water circulation is not always maintained and the saline water flow may be entirely toward the lake. After an instantaneous drop, all saline water flows toward the lake, and only after a certain period of time is the circulation reestablished (Figure 4c). The transition zone characteristic time is defined as the time it takes for the saline water circulation to begin again. More precisely, it is the time at which the inflow to the aquifer at the lake boundary is greater than 0. The circulation reestablishment can indicate the state of the transition zone: When the transition zone is close to equilibrium it does not

Table 3. Parameters for the Sensitivity Test Simulations[a]

Parameter	Value	Other Parameters	τ_{gw} From Simulation (years)	Calculated τ_{gw} (years)	A (m^2 s^{-1}) From Simulations	τ_{TZ} From Simulation (years)
S (1.99E-4)	1.05E-03		15.87	15.76	1.26E-05[b]	10
	9.52E-03		16.29	15.76	1.26E-05	11
n (0.2)	0.1		8.06	7.86	1.26E-05	5
	0.25		19.47	19.62	1.26E-05	12.5
	0.3		23.04	23.54	1.26E-05	15
L (2000)	2500	K = 4.91e-5 h_0 = 40	11.15	11.03	1.96E-05	7
	3000	K = 4.91e-5 h_0 = 40	15.15	15.88	1.74E-05	7.5
	4000	K = 4.91e-5 h_0 = 40	24.45	28.24	1.36E-05	8.5
	4000	Q = 3e-5 K = 9.81e-5 h_0 = 40	14.12	14.12	2.64E-05	4
	5000	K = 4.91e-5 h_0 = 40	39.00	44.12	1.02E-05	9.5
	5000	n = 0.3 K = 4.91e-5 h_0 = 40	50.00	66.17	1.19E-05	12
	5000	n = 0.3 h_0 = 40	331.00	330.87	1.64E-06	8
	20000	K = 4.91e-5 h_0 = 40	706.00	706.00	2.35E-06	16
Δh (10)	1		15.75	15.70	1.14E-06	1
	1.5		15.75	15.70	1.43E-06	1.5
	2.5		15.74	15.70	2.56E-06	3
	5		15.53	15.70	5.32E-06	5
	7		15.53	15.70	7.71E-06	6.5
Q_0 (8.2E-6)	6.00E-06		15.96	15.70	1.10E-05	11
	1.00E-05		15.25	15.70	1.10E-05	9
	1.50E-05		15.25	15.70	1.10E-05	8
	2.00E-05		14.66	15.70	1.10E-05	6.5
	2.50E-05		14.0	15.70	1.10E-05	6.5
K (9.91E-6)	9.81E-07	Q_0 = 8.2E-7	157.00	156.89	7.18E-07	45
	1.96E-06	Q_0 = 8.2E-7	80.00	78.44	7.07E-07	53
	4.90E-06	n = 0.3 Q_0 = 4.1E-6 h_0 = 90	48.16	47.08	5.26E-06	27
	9.81E-06	h_0 = 40	29.12	35.00	4.51E-06	5.5
	1.96E-05	h_0 = 40	14.53	17.65	1.06E-05	6.75
	3.43E-05	h_0 = 40	9.73	10.09	1.77E-05	6
	4.91E-05	h_0 = 40	7.06	7.06	2.43E-05	5
	6.87E-05	h_0 = 40	5.00	5.04	3.66E-05	3.5
h_0 (90)	50		27.00	28.24	6.80E-06	8
	70		22.69	20.17	8.93E-06	10
	100		14.00	14.12	1.27E-05	10
	110		13.59	12.84	1.34E-05	10
	120		12.90	11.77	1.42E-05	10
α_L (10)	5		15.75	15.70	1.10E-05	11
	20		15.75	15.70	1.10E-05	10
	50		15.75	15.70	1.10E-05	9
	50	α_T = 0.05	15.75	15.70	1.10E-05	7
	100		15.75	15.70	1.10E-05	8
	100	α_T = 0.1	15.75	15.70	1.10E-05	5
α_T (0.01)	0.008		15.75	15.70	1.10E-05	10.75
	0.05		15.75	15.70	1.10E-05	9
	0.1		15.75	15.70	1.10E-05	8
	0.5		15.75	15.70	1.10E-05	6
	1		15.75	15.70	1.10E-05	5
K_{max}/K_{min} (20)	10	h_0 = 40	30.20	35.00	4.49E-06	6
	50	h_0 = 40	29.12	35.00	4.49E-06	7
	100	h_0 = 40	31.30	35.00	4.38E-06	8
	200	h_0 = 40	34.51	35.00	3.71E-06	8
ρ_s (1230)	1000		15.80	15.70	8.69E-06	
	1050		15.80	15.70	9.00E-06	8
	1100		15.80	15.70	9.32E-06	10
	1150		15.01	15.70	1.05E-05	11
	1180		14.89	15.70	1.08E-05	11
	1200		15.56	15.70	1.08E-05	10
	1250		15.75	15.70	1.16E-05	10
	1300		15.90	15.70	1.20E-05	10

[a]The parameters are those of the base simulation (Table 2 and in parentheses beneath the parameter symbol) unless mentioned otherwise.
[b]Read 1.26E-05 as 1.26×10^{-5}.

move toward the lake, and therefore enables an inflow of saline water. As stated previously, the expression for the transition zone characteristic time is a function of τ_{gw} and of the hydraulic gradient, which is proportional to K_{max}/Q_0. Furthermore, the dispersivity also affects the response rate of the transition zone. Since high dispersivities cause high velocities in steady state, the saline water circulation reestablishes faster. The anisotropy also affects the response rate of the transition zone because large anisotropy causes smaller vertical velocities [*Voss*, 1999] and a shallower transition zone [*Meisler et al.*, 1985]. However, the effect of the anisotropy in the tested value range (Table 2) was found to be negligible.

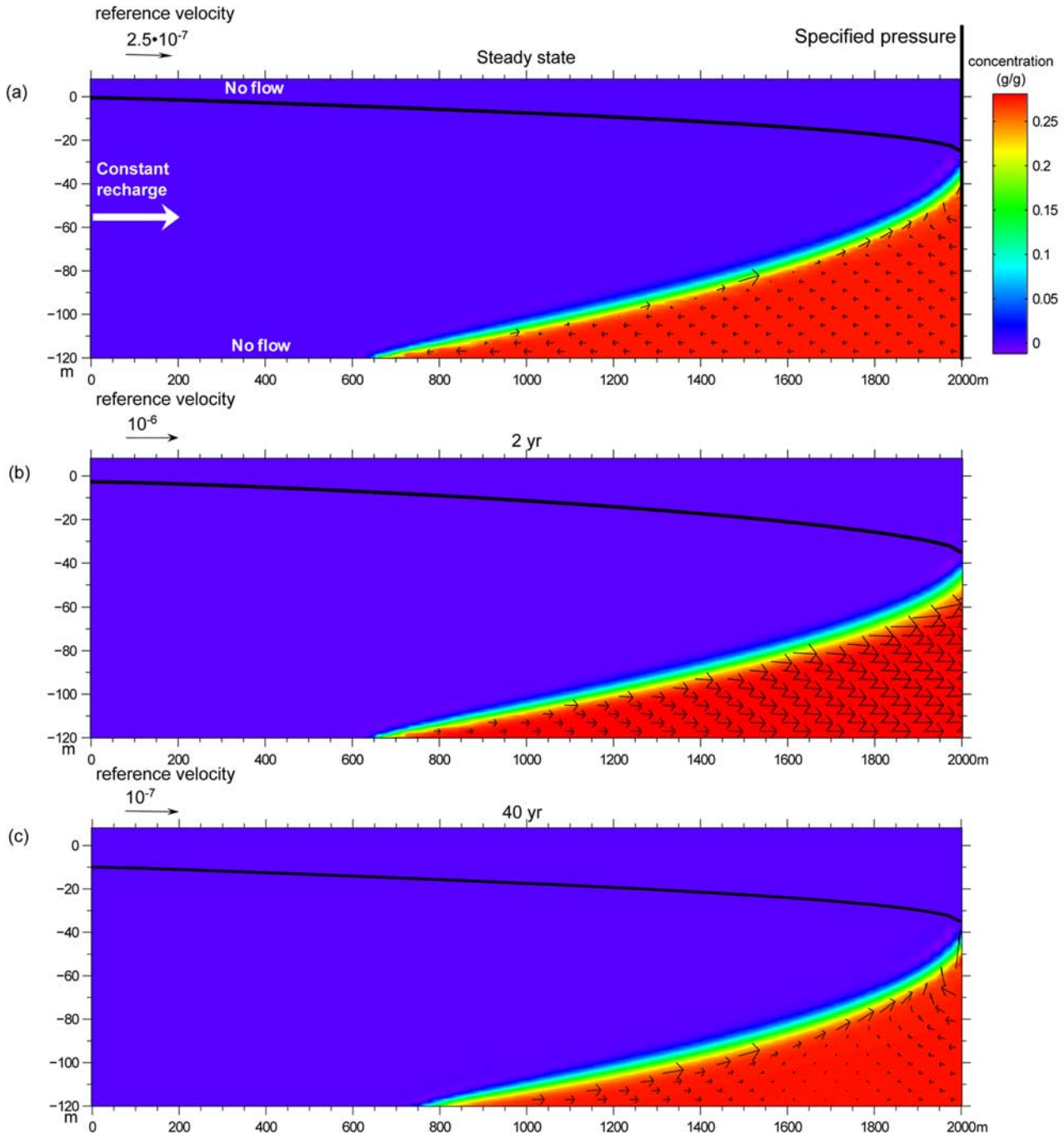

Figure 4. Saline water flow after an instantaneous lake level drop; only the velocity of the saline water is given. The parameter values of the presented results are those of the base simulation (Table 2). The steady state conditions are (a) the initial conditions; (b) after the lake level drops the saline water flow is in the direction of the lake; and (c) after a period of time the saline water circulation reestablishes.

[27] On the basis of the discussion above and on the dimensions of the parameters, the best fit between the characteristic time and the parameters according to the sensitivity tests yields a transition zone characteristic time (τ_{TZ}) given by

$$\tau_{TZ} = \tau_{gw}\frac{K_{\max}h_0^2\Delta h}{Q_0 L^{1.5}(\alpha_L\alpha_T)^{0.25}}\cdot C = \frac{nh_0\sqrt{L}\Delta h}{Q_0(\alpha_L\alpha_T)^{0.25}}\cdot N, \quad (6)$$

where $N = CF$ and $C = 0.33$ when the saline water circulation reestablishes while using the parameter values detailed in Tables 2 and 3. The characteristic time τ_{TZ} indicates whether the transition zone is close to equilibrium, since a slower movement of the transition zone toward the new equilibrium position allows the reestablishment of the circulation. Figure 6 shows the correspondence between the time calculated with (6) and the time obtained from the simulations.

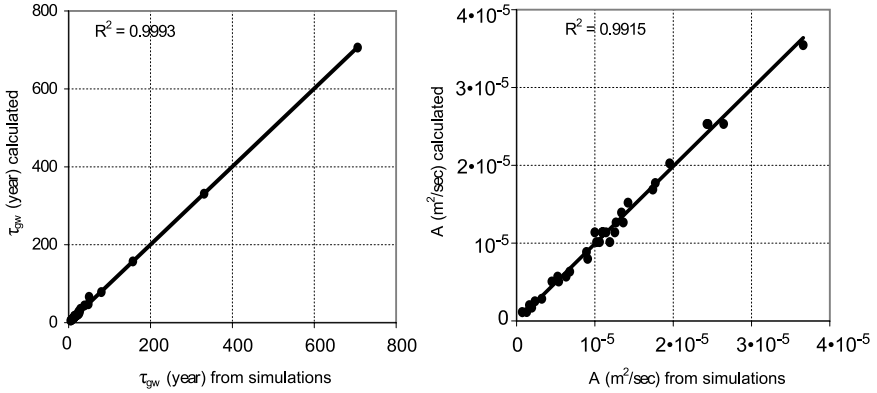

Figure 5. Comparison of the calculated (equation (5)) and simulated water table characteristic times and the coefficient A.

[28] Equation (6) was developed using the Dead Sea region characteristics. It can generally be assumed that in other settings the transition zone response rate in a phreatic aquifer qualitatively depends on the same parameters as in (6). However, the hydraulic conductivity effect is less clear (Table 3, Figure 6), probably due to its effect on both the hydraulic gradient and τ_{gw}. The simulations show that when τ_{gw} is relatively small, τ_{TZ} slightly decreases when the hydraulic gradient increases; when τ_{gw} is relatively large, τ_{TZ} slightly increases when the hydraulic gradient increases, due to the decrease in the hydraulic conductivity (Table 3). Furthermore, when τ_{gw} is large, its effect on τ_{TZ} is smaller. Therefore when τ_{gw} is large the simulated τ_{TZ} are smaller then the calculated τ_{TZ}. This is the reason that in two of the simulations the correspondence between the calculated and simulated τ_{TZ} is weak (Figure 6). A number of simulations were done with varying lake densities that showed that the density has no significant influence on the response rate of the transition zone. In order to quantify the influence of different parameter values, more simulations should be carried out.

[29] The difference between the response times of the water table and the transition zone causes two types of transition zone movement: (1) back and forth movement and (2) gradual movement of the transition zone only toward the lake. The first movement occurs when the water table responds relatively slowly (large τ_{gw}) and the transition zone responds rapidly (small τ_{TZ}). The second type of movement occurs in all other cases. In contrast to previous studies [*Essaid*, 1990; *Harrar et al.*, 2001; *Meisler et al.*, 1985], the transition zone response is not always much slower than the groundwater level response. A steep hydraulic gradient and large τ_{gw} can cause a relatively fast response of the transition zone, as they cause a relatively steep slope in the transition zone and thus a strong lateral density gradient.

[30] The magnitude of the saline water velocities in the direction of the lake and the rate of flow direction change depend on the rate of the transition zone response. Large values of τ_{TZ} induce small velocities in the direction of the lake and a slow change in flow direction of the saline water.

4. Groundwater Response to a Continuous Base Level Drop

[31] The second stage of this work examines the case of a continuous drainage base level drop. In this case we can solve (1) with boundary and initial conditions representing a continuous level drop: $h(0, t) = Rt$; $\frac{\partial h}{\partial x}(L, t) = \frac{Q_0}{T}$; $h(x, 0) = \frac{Q_0}{T}x$, where R [L/T] is the rate of the level drop. Note that the linearization assumption is reasonable only when the total drop of the base level is considerably smaller than the thickness of the flow section.

[32] The solution of (1) with the boundary conditions above can be obtained from (2) by superposition following the Duhamel method [*Courant and Hilbert*, 1953]:

$$h(x,t) = \frac{Q_0}{T}x - \frac{2nL^2R}{T}\sum_{k=0}^{\infty}\frac{1}{(\pi/2+\pi k)^3}\sin\left(\frac{\pi/2+\pi k}{L}x\right) \cdot \left(1 - e^{-\frac{T}{nL^2}(\pi/2+\pi k)^2 t}\right). \quad (7)$$

After applying Darcy's law, the discharge at $x = 0$ is

$$Q(0,t) - Q_0 = 2nLR\sum_{k=0}^{\infty}\frac{1}{(\pi/2+\pi k)^2}\left(1 - e^{-\frac{T}{nL^2}(\pi/2+\pi k)^2 t}\right). \quad (8)$$

Figure 7 presents the analytical calculated discharge together with results of numerical simulations. Some disagreements between analytical and numerical results are related to the effects of linearization and circulation in

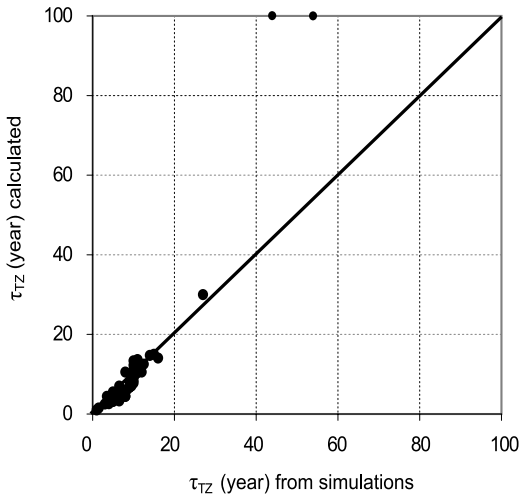

Figure 6. Comparison of the calculated (equation (6)) and simulated τ_{TZ}.

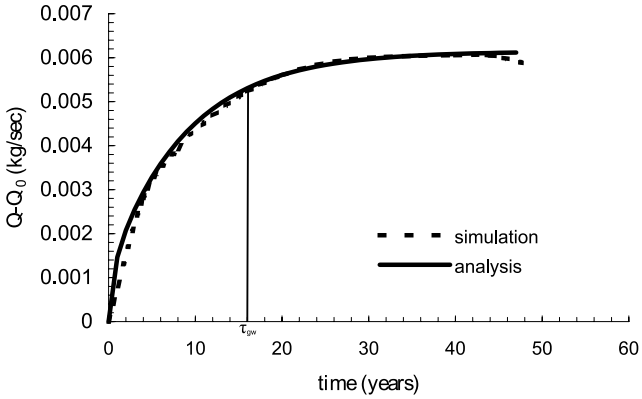

Figure 7. Change in the discharge versus time when the lake level drops continuously. The parameter values of the presented results are those of the base simulation (Table 2) with $R = 0.5$ m a^{-1}.

the saline water body beneath the moving transition zone. Note that the flow section thickness (h_0), which changes during the drop of the base level, is approximated to be constant and was taken as the minimal flow section thickness during the simulation.

[33] The theoretical results (8) and the simulation results show that the groundwater discharge at the lake boundary increases until it attains a constant value that is higher than the inflow value (Figure 7). At this time the groundwater system has attained a new dynamic equilibrium in which the water table drops (Figure 8) but the hydraulic gradient remains constant. In the first stage, when the discharge increases, the hydraulic gradient increases until the new dynamic equilibrium is attained, in which the hydraulic gradient becomes constant and larger than its initial value. The discharge plot as a function of time (Figure 7), calculated using (8), can be used to estimate the stage that a given groundwater system has reached (Figure 7). Knowing the elapsed time since the drop began will give the groundwater discharge that is expected with a given set of parameters.

[34] The saline water beneath the transition zone initially circulates, because the lake level is still close to equilibrium. After a certain period of time, the saline water flow turns toward the lake, and after the new dynamic equilibrium has been reached the circulation gradually reestablishes in some cases (Figure 9). The factors that control the circulation reestablishment are τ_{gw}, the dispersivity, the anisotropy, and τ_{TZ}. During the lake level drop, two processes control the saline water flow direction: (1) the drop of the lake level, which causes saline water flow toward the lake, and (2) the dispersive process, which causes an inflow of saline water due to the saline water discharge in the transition zone. Calculating τ_{TZ} of a given system gives an estimate of the response rate of the transition zone. Furthermore, the value of τ_{TZ}, according to (6), indicates the time when the saline water changes its flow direction.

5. Application to Wadi Arugot Alluvial Fan in the Dead Sea Area

5.1. Field Data

[35] The water table and the location of the transition zone were monitored in the alluvial fan of Wadi Arugot over the past 3 years, during the Dead Sea level drop. The site extends for about 2 km from the shoreline inland (Figure 2). The transition zone location was monitored by electric conductivity (EC) profiles in the boreholes. The relation between the water EC and salinity in the Dead Sea is linear up to the salinity of normal seawater. Above this salinity, up to two thirds of the salinity of the Dead Sea, the relation is nonlinear. Beyond this value the relation is a double-valued function and cannot be defined [*Yechieli*, 2000].

[36] The water table has dropped during the past 3 years in all of the boreholes at the same rate as that of the Dead Sea level (Figures 1 and 8), keeping the hydraulic gradient constant. Coinciding with the drop in the water table, the transition zone has also dropped and widened during the past 3 years (Figure 10). Furthermore, the drop in the Dead Sea has been accompanied by a change in its chemical composition: The Na/Cl ratio has decreased and the Mg/K ratio has been increased during the past 40 years [*Gavrieli*, 1997]. This composition change was also detected in groundwater samples from boreholes. The Na/Cl ratio decreases with depth and in the direction of the Dead Sea, implying that the saline groundwater is Dead Sea water, whose age decreases with depth and proximity to the lake [*Kiro*, 2006].

5.2. Simulations for Wadi Arugot

[37] The aquifer in the Dead Sea area is composed of gravel with a small amount of clay and silt. Thus the simulation parameters are set to represent a gravel medium (Table 4). The main parameters estimated were the inflow from the western boundary and the permeability of the aquifer. The inflow can be approximated from the estimated discharge of the springs in this area, which is 10^6 to 5×10^6 m^3 a^{-1} km^{-1}. Independent simulations of groundwater flow toward the En-Gedi area also yielded an estimated

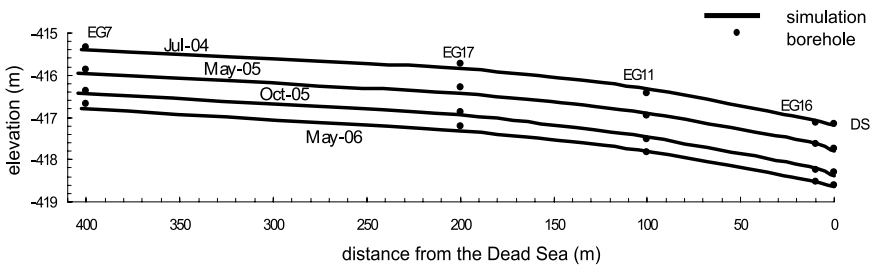

Figure 8. Comparison of the groundwater levels measured in boreholes during the past few years with the simulation results.

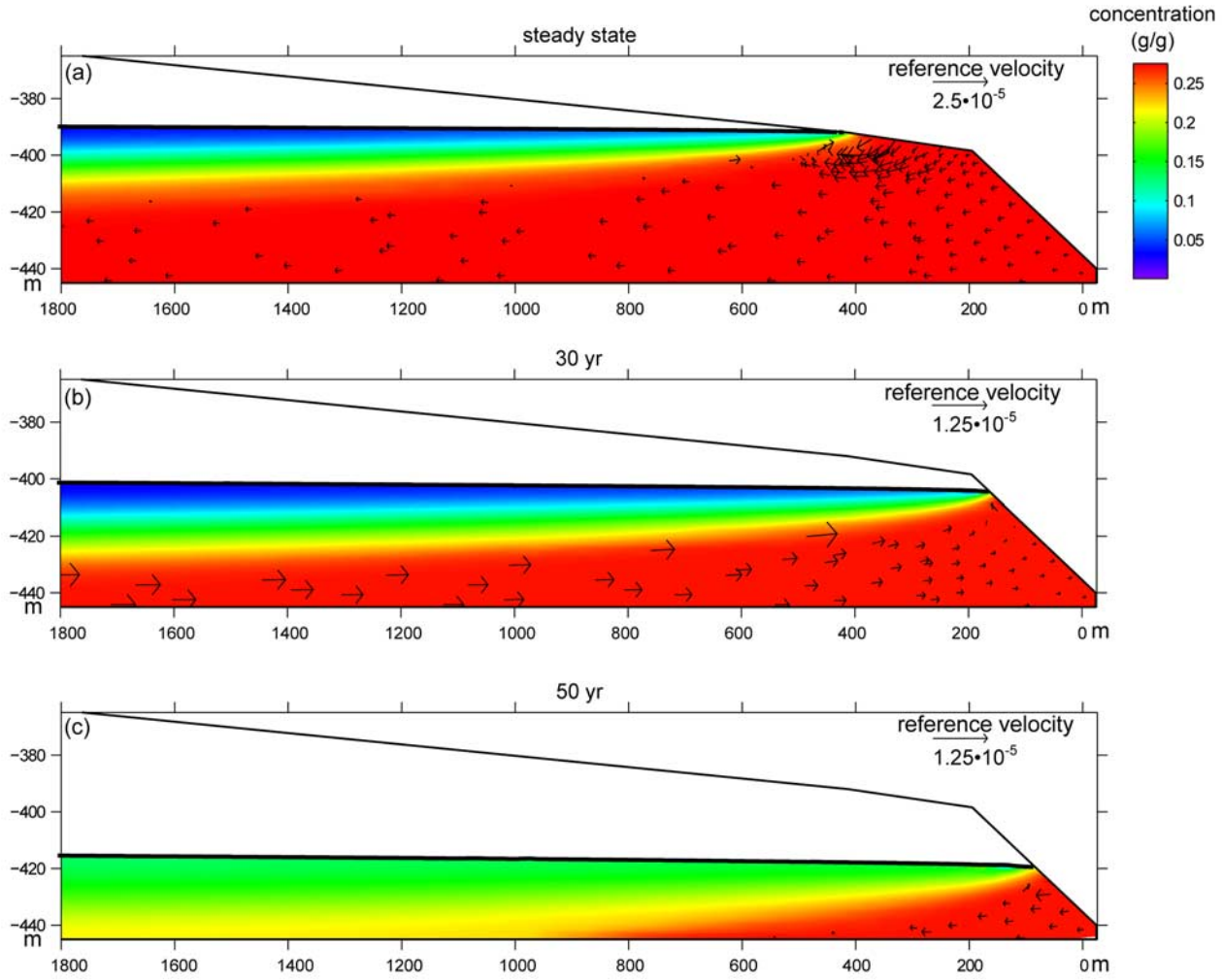

Figure 9. Simulation results of the transition zone movement, groundwater levels, and saline water flow during the Dead Sea level drop at Wadi Arugot. The parameter values are those that create the smallest hydraulic gradient in the range of the parameter estimation ($k = 4 \times 10^{-10}$ m^2 and $Q_0 = 0.03$ kg s^{-1}). The remainder of the parameters are detailed in Table 4, and the topography and bathymetry are those of Wadi Arugot. Steady state conditions are given in Figure 9a. The western boundary with the fresh water inflow is about 25 km westward since the transition zone must not intersect with this boundary. Only the saline water velocities are shown. The transition zone widens during the Dead Sea level drop (Figures 9b and 9c). The saline water flow is in the direction of the aquifer most of the time (Figure 9c).

inflow of about 3×10^6 m^3 y^{-1} km^{-1} [*Laronne*, 2003]. We assume that there are no seasonal changes in the recharge. Previous studies, however, do suggest a seasonal response of groundwater to the increase of the Dead Sea level [*Yechieli et al.*, 1995]. The seasonal changes of the inflow can be neglected compared with the Dead Sea level changes because of the arid climate of the Dead Sea. It can be assumed that due to the distance from the Judean Mountains (30 km), which are the source of freshwater in the Dead Sea region, the seasonal changes in the source are averaged over time. No seasonal changes in spring discharge in the region are known, and *Yechieli et al.* [1995] show that during the winter the water table near the shore responds faster and more significantly than groundwater near the freshwater source. The permeability is estimated from pumping tests [*Wollman et al.*, 2003] to be 1.3×10^{-11} to 4×10^{-10} m^2. According to Darcy's law, at steady state the hydraulic gradient in the research area should be between the two extremities that this range of parameter values defines.

[38] The boundary conditions are the same as those in Table 1. The historic Dead Sea level drop is imposed at the eastern boundary, and the shape of the domain conforms to the topography and bathymetry of the research area. Note that in this case the boundary is not vertical. The location of the lower boundary is set by a layer of low permeability in the aquifer that is at an elevation of −445 m. The initial conditions are water table and transition zone in equilibrium with the Dead Sea level, as it was 50 years ago.

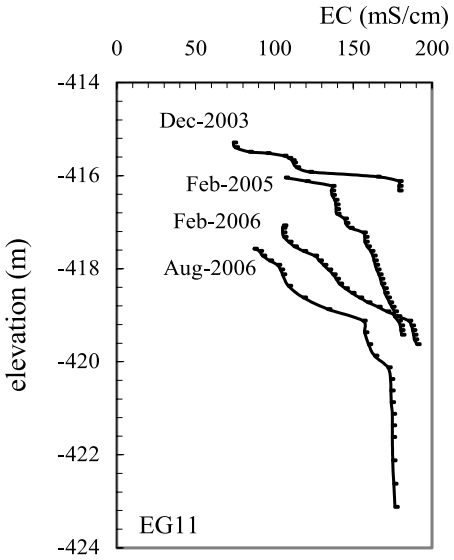

Figure 10. Electric conductivity profiles in the EG11 borehole during the past 3 years.

[39] The distance between the western boundary and the Dead Sea is at least 2 km. In the small hydraulic gradient simulations the length of the aquifer is extended to up to 25 km because of constraints of the boundary conditions. Because of the western boundary condition of the freshwater inflow, it is not possible to intersect the transition zone with this boundary. A fresh water inflow into the transition zone would cause mixing and widening of the transition zone, which would not represent correctly the processes in the research area. This issue needs to be considered because the length of the model affects the response of the groundwater system, as we showed previously. Nonetheless, we assume that the effect of the aquifer length on the water table and the transition zone near the shore is minor. Calculating the characteristic time with the actual aquifer length can be used as a correction for the discharge to the lake.

[40] The simulation results that most closely fit the field data are those with the smallest hydraulic gradient ($k = 4 \times 10^{-10}$ m^2, $Q_0 = 0.03$ kg s^{-1}). The difference between the simulation results and their characteristic times demonstrates two types of behavior of the groundwater system, with respect to the response rates. In the small gradient simulation $\tau_{gw} = 0.1$ year for an aquifer length of 2 km. Hence the new dynamic equilibrium occurred a few months after the Dead Sea started to drop. In the large hydraulic gradient simulations $\tau_{gw} = 3.55$ years, indicating that the hydraulic gradient becomes significantly larger with time but at a slower rate. Moreover, the transition zones in both simulations behave very differently. Because of the small hydraulic gradient (large τ_{TZ}), the transition zone response is slower compared with the water table response. This leads to a very wide and dispersive transition zone (Figure 9). In the large hydraulic gradient simulation, τ_{TZ} is smaller, leading to a transition zone that is always in equilibrium with the water table (Figure 11).

[41] Because of the relatively slow movement of the transition zone when the hydraulic gradient is small, the transition zone is very dispersive and becomes wider with time (Figure 9). Furthermore, the effect of the vertical movement on the transition zone thickness is also noticeable. When the boundary is steeper due to the different topography, the vertical flow component of the groundwater due to the lake level drop is more significant. Therefore the longitudinal dispersivity component is closer to being perpendicular to the transition zone and widens the transition zone more significantly (Figure 9).

5.3. Comparison of Simulation Results and Field Data

[42] While the values of the parameters k and Q_0 lead to different types of groundwater system behavior, the abundance of field data in the research area and independent observations can lead to a good estimation of their values. The groundwater levels in the boreholes constrain the initial hydraulic gradient to be smaller than the present hydraulic gradient in the field, since it increases during the drop of the lake level. Comparing the hydraulic gradient in the field with the simulation results together with the parameters estimated from the independent measurements detailed above narrows the parameter range significantly. Furthermore, the shape of the transition zone, which is also affected by the hydraulic gradient, also constrains these parameters.

[43] The geochemical data also constrain the aquifer parameters by indicating a continuous lateral flow of Dead Sea water into the aquifer during the drop of the lake level

Table 4. Parameters for Dead Sea Simulations (Isothermal Conditions)

Parameter	Unit	Value	Reference
Aquifer compressibility	$[\text{kg}/(\text{m s}^2)]^{-1}$	10^{-10}	calculated from the bulk modulus [*Maimon et al.*, 2005]
Fluid compressibility	$[\text{kg}/(\text{m s}^2)]^{-1}$	4.47×10^{-10}	*Freeze and Cherry* [1979]
Horizontal permeability	m^2	1.3×10^{-11} to 4×10^{-10}	pumping test [*Wollman et al.*, 2003]
Vertical permeability	m^2	4×10^{-12}	anisotropy in a layered medium [*Freeze and Cherry*, 1979]
Porosity		0.2	typical for nonhomogenous gravel [*Davis*, 1969]
Fluid viscosity[a]	kg (m s)$^{-1}$	0.001	*Freeze and Cherry* [1979]
Freshwater density (ρ_0)	kg m^{-3}	1000	*Freeze and Cherry* [1979]
Freshwater concentration (C_0)		0	
Groundwater density	kg m^{-3}	$\rho = \rho_0 + \partial\rho/\partial C(C - C_0)$	
Density change with concentration ($\partial\rho/\partial C$)		836	
Dead Sea water concentration		0.275	*Neev and Emery* [1967]
Longitudinal dispersivity	m	10	typical for gravel [*Gelhar et al.*, 1992]
Transverse dispersivity	m	0.1	typical for gravel [*Gelhar et al.*, 1992]
Inflow	kg s^{-1}	0.03–0.16	spring discharges, independent simulations [*Laronne*, 2003]

[a]The viscosity of the Dead Sea is 3 times that of fresh water. This issue is not considered in this study.

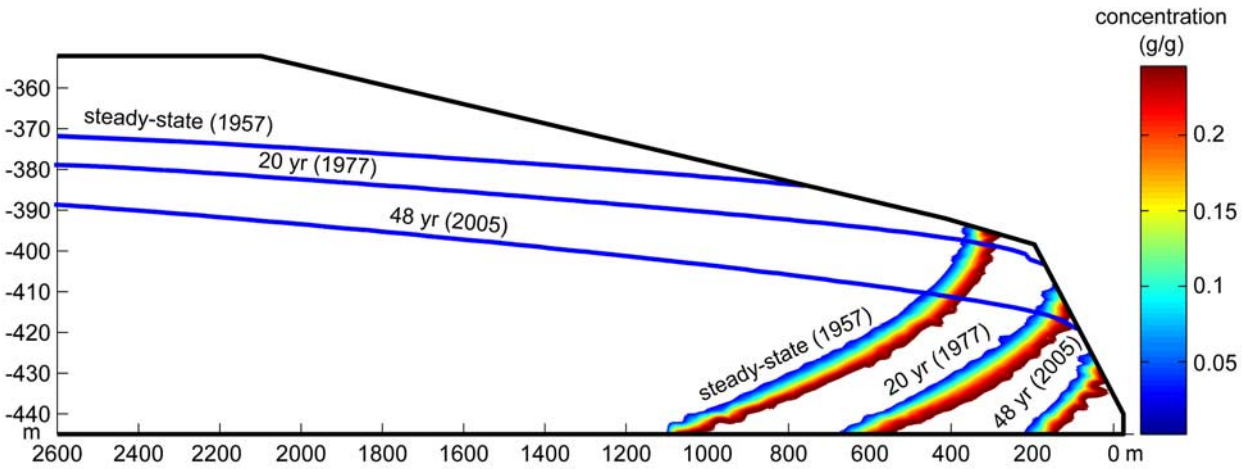

Figure 11. Simulation results with a relatively large hydraulic gradient (Table 4; $k = 1.3 \times 10^{-11}$ m^2; $Q_0 = 0.06$ kg s^{-1}).The hydraulic gradient increases considerably, and the transition zone moves relatively fast and is always in equilibrium with the water table.

[*Kiro*, 2006]. That is, the parameter values must allow a saline water circulation or partial circulation during most of the Dead Sea level drop. Additionally, the geochemical observations constrain the dispersivities, which affect the transition zone thickness and the saline water circulation. Therefore the concentration profiles and the continuous lateral flow of saline water observed in the field also constrain the dispersivity values.

[44] A good fit between the simulation results and the field data is obtained with the parameters that produce the smallest hydraulic gradient: $k = 4 \times 10^{-10}$ m^2 and $Q_0 = 0.03$ kg s^{-1} (10^3 m^3 a^{-1}). Applying these values, there is a good correspondence of the water table (Figure 8) and the concentration profiles (Figure 12). The longitudinal and transverse dispersivities that fit the concentration profiles in the boreholes and enable circulation are 10 m and 0.1 m, respectively. Larger dipersivities affect the transition zone shape [*Voss*, 1999], and smaller dispersivities do not enable an inflow of saline water. These dispersivities are typical of an alluvial aquifer according to *Gelhar et al.* [1992]. Figures 8 and 12 demonstrate the simulation's

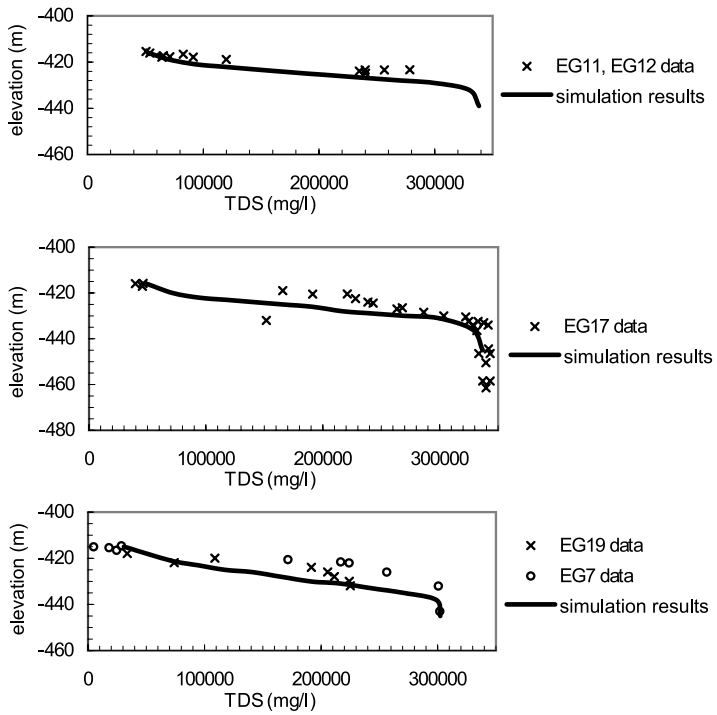

Figure 12. Comparison between simulation results of Figure 9 and field data, showing correspondence between the salinity in the field data and the concentration calculated from the simulation (data from *Kiro* [2006]).

suitability to represent the groundwater system in the research area.

6. Discussion

6.1. The Characteristic Times

[45] On the basis of mathematical analysis of the linearized 1-D equation and series of 2-D numerical simulations, we derived relationships for the groundwater characteristic time (τ_{gw}) and the discharge coefficient (A). According to (8), the time period to attain the new dynamic equilibrium depends only on the aquifer parameters. However, the magnitude of the discharge in the new equilibrium is proportional to nLR assuming that the aquifer thickness B and h_0 have almost the same value and cancel out one another. Therefore the water volume discharging to the lake during any given time interval after the new dynamic equilibrium is attained is the water volume bounded between two water tables during this time interval plus the inflow Q_0. Therefore a larger rate of lake level drop increases the discharge.

[46] The effect of the hydrological parameters on τ_{TZ} is more complicated. Unlike $\tau_{gw,}$ τ_{TZ} is affected by anisotropy and dispersivity. High dispersivity and low anisotropy tend to create saline water circulation despite the lake level drop. In addition, τ_{TZ} is also affected by the hydraulic gradient. High hydraulic gradients cause a large slope in the transition zone, which in turn causes a high-density gradient and subsequently causes a rapid response of the transition zone. The aquifer thickness B also affects the time at which the saline water circulation reestablishes (equation (6)) since large aquifer thickness implies a large body of saline groundwater that is more balanced in its inflows and outflows. In other words, when B is small, any saline outflow is a large portion of the volume of the saline water that must be compensated for by an inflow of saline water into the aquifer.

6.2. Patterns of Groundwater Flow

[47] The response of the groundwater system to a continuous lake level drop strongly depends on the characteristic times of the system. Several typical scenarios are noted:

[48] 1. One scenario is a system always in equilibrium with the lake level when the characteristic times are small. A small τ_{gw} indicates a quick establishment of the new dynamic equilibrium. An increase in the lake level drop rate R leads to an increase in the new discharge and the new hydraulic gradient. Small τ_{TZ} causes a fast response of the transition zone that is always in equilibrium with the water table.

[49] 2. Another is a system far from equilibrium with the lake level when the characteristic times are large. The system requires a long period of time to attain the new dynamic equilibrium. The hydraulic gradient and the discharge might not increase significantly if the rate of the lake level drop is relatively slow.

[50] 3. Still another is a system in which one characteristic time is relatively small and the other is relatively large. This includes two cases: (1) large τ_{gw} and small τ_{TZ} (in this case the hydraulic gradient tends to increase with time and the transition zone tends to be in equilibrium with the water table (Figure 11)); and (2) small τ_{gw} and a large τ_{TZ} (in this case the water table tends to be in equilibrium with the lake level and the transition zone is still far from equilibrium (Figure 9)).

[51] There are a few factors that control the saline water flow direction during a lake-level drop.

6.2.1. Change in the Shoreline Location

[52] In most cases the boundary where a level drop occurs is not vertical. Thus the lake does not only move vertically, it also moves horizontally, and the transition zone moves toward the lake in order to reach equilibrium. This horizontal movement causes a flow of saline water toward the lake. Slower movement of the transition zone (large τ_{TZ}) causes a saline water flow tendency toward the lake, as in the small hydraulic gradient results. However, this process enables partial circulation during a drop in the lake level, since there is still an outflow of saline water due to hydrodynamic dispersion (Figure 9b).

6.2.2. Head Differences at the Boundary due to the Lake Level Drop

[53] A drop in the lake level causes a head difference near the boundary. At the boundary the head drop is immediate, but in a porous medium the groundwater response is delayed. This head difference drives a saline water outflow toward the lake. In this case, the saline water near the boundary flows toward the lake, while the saline water velocities far from the boundary might be in the opposite direction. This process is significant when the permeability is small.

6.2.3. Changes in the Hydraulic Gradient

[54] During a lake level drop, the hydraulic gradient becomes larger until the new dynamic equilibrium is reached. If the transition zone responds quickly to the change in the hydraulic gradient (small τ_{TZ}), it moves toward the lake. It has been shown that the recharge and hydraulic gradient increase due to seasonal changes lead to an increase in the discharge to the sea [*Michael et al.*, 2005]. This process is significant when the transition zone moves relatively fast (small τ_{TZ}) and the water table responds relatively slowly (large τ_{gw}).

6.2.4. Hydrodynamic Dispersion

[55] The hydrodynamic dispersion's effect on the saline water velocity in steady state is similar during a lake level drop. The saline water flow tends to circulate when the dispersivities are high. This process is independent of the other processes.

6.2.5. Anisotropy

[56] Low anisotropy values enable vertical flow and saline water circulation in steady state [*Voss*, 1999]. During a lake level drop, the saline water velocity tends to be in the direction of the lake when the anisotropy is high.

7. Summary and Conclusions

[57] The results of this study lead to several conclusions, some of which apply to base level drops in general and others are specific to the case of the Dead Sea region. The combination of the theoretical analysis, the simulations, and the field data provides a robust theory.

7.1. General

[58] 1. Two characteristic times, that of the water table response (τ_{gw}) and that of the transition zone response (τ_{TZ}), were defined by theoretical analysis and validated by

simulations. A relation between the hydrologic parameters and these characteristic times was developed.

[59] 2. The transition zone response time could be different from the water table response time because it depends also on the hydraulic gradient. Thus, in contrast to reports of previous studies, when the hydraulic gradient is relatively large, the transition zone may respond relatively fast and remain in equilibrium with the water table.

[60] 3. The saline water flow direction during a base level drop can be in the direction of the lake or can circulate as in steady state.

[61] 4. During a continuous base level drop, the discharge to the lake and the hydraulic gradient increase until a new dynamic equilibrium is reached, in which the discharge and the hydraulic gradient remain constant. The value of τ_{gw} represents the time required to attain the new equilibrium. The magnitude of the discharge and the hydraulic gradient in the new dynamic equilibrium is proportional to the porosity, to the boundary distance from the shore, and to the lake level drop rate.

[62] 5. The saline water circulation that occurs in steady state tends to reestablish when the new equilibrium is attained.

[63] 6. Because of the vertical movement of the transition zone due to the lake level drop, the longitudinal dispersivity causes a widening of the transition zone. Therefore the bathymetry of the lake affects the width of the transition zone. Steep bathymetry, which causes a more significant vertical movement, will widen the transition zone more significantly.

7.2. Specific to the Dead Sea Research Area

[64] Field data and simulations indicate the following:

[65] 1. The water table in Wadi Arugot drops fast (1 m a^{-1}) and has reached a new dynamic equilibrium in which the hydraulic gradient is constant, keeping the water table parallel up to 2 km from the shore.

[66] 2. The transition zone in the research area drops fast, causing flushing of the saline water at a fast rate. However, it moves more slowly than the water table and becomes wider with time due to the small hydraulic gradient.

[67] 3. There is a lateral westward flow of Dead Seawater into the aquifer despite the drop of the lake level.

[68] 4. The correspondence between field data and simulation results regarding salinity profiles and water tables leads to a robust estimation of the parameters and enables predicting the behavior of the groundwater system in the future.

[69] **Acknowledgments.** We thank H. Hemo for the field data collection and D. Feldman and S. Kiro for their assistance. We also thank the reviewers for their many constructive comments that improved this paper significantly. We thank E. Kagan for proofreading the manuscript. This research was supported by Israel Science Foundation grant ISF 479/03.

References

Anati, A. D., and S. Shasha (1989), Dead Sea surface level changes, *Isr. J. Earth Sci.*, *16*, 181–196.

Anderson, M. P., and X. Cheng (1993), Long- and short-term transience in a groundwater/lake system in Wisconsin, USA, *J. Hydrol. Amsterdam*, *145*, 1–18, doi:10.1016/0022-1694(93)90217-W.

Arad, A., and A. Michaeli (1967), Hydrogeological investigations in the western catchment of the Dead Sea, *Isr. J. Earth Sci.*, *16*, 181–196.

Ataie-Ashtiani, B., R. E. Volker, and D. A. Lockington (1999), Tidal effects on sea water intrusion in unconfined aquifers, *J. Hydrol. Amsterdam*, *216*, 17–31, doi:10.1016/S0022-1694(98)00275-3.

Bear, J. (1972), *Dynamics of Fluids in Porous Media*, 764 pp., Elsevier, New York.

Bear, J. (1979), *Hydraulics of Groundwater*, 569 pp., McGraw-Hill, New York.

Bush, W. P. (1988), Simulation of saltwater movement in the Floridan aquifer system, Hilton Head Island, South Carolina, *U.S. Geol. Surv. Water Supply Pap.*, *2331*, 19 pp.

Chen, B. F., and S. M. Hsu (2004), Numerical study of tidal effects on seawater intrusion in confined and unconfined aquifers by time-independent finite-difference method, *J. Waterw. Port Coastal Ocean Eng.*, *130*, 191–206, doi:10.1061/(ASCE)0733-950X(2004)130:4 (191).

Cherkauer, D. S., and J. P. Zager (1989), Groundwater interaction with a kettle-hole lake: Relation of observations to digital simulations, *J. Hydrol. Amsterdam*, *109*, 167–184, doi:10.1016/0022-1694(89)90013-9.

Cooper, H. H. (1959), A hypothesis concerning the dynamic balance of fresh water and salt water in a coastal aquifer, *J. Geophys. Res.*, *64*, 461–467, doi:10.1029/JZ064i004p00461.

Courant, R., and D. Hilbert (1953), *Methods of Mathematical Physics*, 1st ed., 830 pp., Wiley-Interscience, New York.

Crank, J. (1975), *The Mathematics of Diffusion*, 2nd ed., 414 pp., Clarendon, Oxford, U.K.

Davis, S. N. (1969), Porosity and permeability of natural materials, in *Flow Through Porous Media*, edited by R. J. M. DeWiest, pp. 53–89, Academic, San Diego, Calif.

Essaid, H. I. (1990), A multilayered sharp interface model of coupled freshwater and saltwater flow in coastal systems: Model development and application, *Water Resour. Res.*, *26*, 1431–1454.

Freeze, R. A., and A. J. Cherry (1979), *Groundwater*, 604 pp., Prentice-Hall, Upper Saddle River, N. J.

Gavrieli, I. (1997), Halite deposition from the Dead Sea; 1960–1993, in *The Dead Sea; the Lake and Its Setting*, edited by T. M. Niemi et al., pp. 161–170, Oxford Univ. Press, New York.

Gelhar, L. W., C. Welty, and K. R. Rehfeldt (1992), A critical review of data on field-scale dispersion in aquifers, *Water Resour. Res.*, *28*, 1955–1974, doi:10.1029/92WR00607.

Harrar, W. G., A. T. Williams, J. A. Barker, and M. V. Camp (2001), Modelling scenarios for the emplacement of palaeowaters on aquifer systems, in *Palaeowaters in Coastal Europe: Evolution of Groundwater Since the Late Pleistocene*, edited by W. M. Edmunds and C. J. Milne, *Spec. Publ. Geol. Soc. London*, *189*, 213–229.

Kiro, Y. (2006), The effect of the Dead Sea level drop in the past 50 years on the groundwater system in the alluvial aquifer in its vicinity, M.S. thesis, 116 pp., Hebrew Univ. of Jerusalem, Jerusalem, Israel.

Klein, C., and A. Flohn (1987), Contribution to the knowledge in the fluctuations of the Dead Sea level, *Theor. Appl. Climatol.*, *38*, 151–156, doi:10.1007/BF00868099.

Kohout, F. A. (1960), Cyclic flow of salt water in the Biscayne aquifer of southeastern Florida, *J. Geophys. Res.*, *65*, 2133–2141, doi:10.1029/JZ065i007p02133.

Laronne, L. (2003), Groundwater flow modeling in the eastern Judea Group aquifer, M.S. thesis, 87 pp., Hebrew Univ. of Jerusalem, Jerusalem, Israel.

Lensky, N. G., Y. Dvorkin, V. Lyakhovsky, I. Gertman, and I. Gavrieli (2005), Water, salt, and energy balances of the Dead Sea, *Water Resour. Res.*, *41*, W12418, doi:10.1029/2005WR004084.

Maimon, O., V. Lyakhovsky, A. Agnon, and M. Abelson (2005), *Stability of Cavities and Formation of Sinkholes Along the Dead Sea Coast*, 59 pp., Geol. Surv. of Isr., Jerusalem, Israel.

Meisler, H., P. P. Leahy, and L. L. Knobel (1985), Effect of eustatic sea-level changes on saltwater-freshwater relations in the northern Atlantic coastal plain, *U.S. Geol. Surv. Water Supply Pap.*, *2255*, 28 pp.

Michael, H. A., A. E. Mulligan, and C. F. Harvey (2005), Seasonal oscillations in water exchange between aquifers and the coastal ocean, *Nature*, *436*, 1145–1148, doi:10.1038/nature03935.

Neev, D., and K. O. Emery (1967), The Dead Sea: Depositional process and environments of evaporites, *Bull. Geol. Surv.*, 41.

Rogers, D. B., and S. J. Dreiss (1995), Saline groundwater in Mini Basin, California: 2. Long-term control of lake salinity by groundwater, *Water Resour. Res.*, *31*, 3151–3169, doi:10.1029/95WR02109.

Sacks, L. A., J. S. Herman, L. F. Konikow, and A. L. Vela (1992), Seasonal dynamics of groundwater-lake interactions at Doñana National Park, Spain, *J. Hydrol. Amsterdam*, *136*, 123–154, doi:10.1016/0022-1694(92)90008-J.

Underwood, M. R., F. L. Peterson, and C. I. Voss (1992), Groundwater lens dynamics of atoll islands, *Water Resour. Res.*, *28*, 2889–2902, doi:10.1029/92WR01723.

Voss, C. I. (1984), SUTRA: Finite-element simulation model for saturated-unsaturated, fluid-density-dependent groundwater flow with energy transport or chemically reactive single-species solute transport, *U.S. Geol. Surv. Water Resour. Invest. Rep.*, *84-4369*, 429 pp.

Voss, C. I. (1999), *USGS SUTRA Code: History, Practical Use, and Application in Hawaii*, 625 pp., Kluwer Acad., Dordrecht, Netherlands.

Winter, T. C. (1978), Numerical simulation of steady state three-dimensional groundwater flow near lakes, *Water Resour. Res.*, *14*, 245–254, doi:10.1029/WR014i002p00245.

Wollman, S., Y. Yechieli, V. Lyakhovsky, and A. Bein (2003), *Results of a Pumping Test in Wadi Arugot*, 10 pp., Geol. Surv. of Isr., Jerusalem, Israel.

Yechieli, Y. (1993), The effects of water level changes in closed lakes (Dead Sea) on the surrounding groundwater and country rocks, Ph.D. thesis, 197 pp., Weizmann Inst. of Sci., Rehovot, Israel.

Yechieli, Y. (2000), Fresh-saline groundwater interface in the western Dead Sea area, *Ground Water*, *38*, 615–623, doi:10.1111/j.1745-6584.2000.tb00253.x.

Yechieli, Y., D. Ronen, B. Berkovitz, W. Dershowitz, and A. Hadad (1995), Aquifer characteristics derived from the interaction between water levels of a terminal lake (Dead Sea) and an adjacent aquifer, *Water Resour. Res.*, *31*, 893–902, doi:10.1029/94WR03154.

Y. Kiro and A. Starinsky, Institute of Earth Sciences, Givat Ram, Hebrew University of Jerusalem, Jerusalem 91904, Israel. (yael.kiro@mail.huji.il)

V. Lyakhovsky, E. Shalev, and Y. Yechieli, Geological Survey of Israel, 30 Malkhe Israel Street, Jerusalem 95501, Israel.